Tryptophan mediated photoreduction of disulfide bond causes unusual fluorescence behaviour of *Fusarium solani pisi* cutinase

Jeanine J. Prompers[a,1], Cornelis W. Hilbers[a], Henri A.M. Pepermans[b,*]

[a] *NSR Center for Molecular Structure, Design and Synthesis, Laboratory of Biophysical Chemistry, University of Nijmegen, Toernooiveld, 6525 ED Nijmegen, The Netherlands*
[b] *Unilever Research, Olivier van Noortlaan 120, 3133 AT Vlaardingen, The Netherlands*

Received 4 March 1999; received in revised form 4 July 1999

Abstract The fluorescence signal of the single tryptophan residue (Trp^{69}) of *Fusarium solani pisi* cutinase is highly quenched. However, prolonged irradiation of the enzyme in the tryptophan absorption band causes an increase of the tryptophan fluorescence quantum yield by an order of magnitude. By using a combination of NMR spectroscopy and chemical detection of free thiol groups with a sulfhydryl reagent we could unambiguously show that the unusual fluorescence behaviour of Trp^{69} in cutinase is caused by the breaking of the disulfide bond between Cys^{31} and Cys^{109} upon irradiation, while the amide-aromatic hydrogen bond between Ala^{32} and Trp^{69} remains intact. This is the first example of tryptophan mediated photoreduction of a disulfide bond in proteins.

Key words: Fluorescence spectroscopy; Nuclear magnetic resonance; Thiol; Tryptophan mediated photoreduction; Disulfide bond; Cutinase

1. Introduction

The single tryptophan residue (Trp^{69}) of *Fusarium solani pisi* cutinase exhibits unusual fluorescence behaviour [1]. In the enzyme's native state the tryptophan fluorescence is highly quenched. However, prolonged irradiation of the enzyme in the tryptophan absorption band causes an increase of the tryptophan fluorescence quantum yield by an order of magnitude. This increase was ascribed to a photo-induced, subtle structural change to a species whose fluorescence is not highly quenched [1]. However, the mechanism by which the tryptophan fluorescence is quenched in native cutinase could not be deduced and it was not known how this mechanism would be eliminated upon irradiation.

Cutinases are lipolytic enzymes capable of degrading cutin [2], the insoluble lipid-polyester matrix covering the surface of plants. They are produced by several phytopathogenic fungi and pollen, enabling them to gain entry into the plant by enzymatic digestion of its cuticle. Moreover, these enzymes, like lipases, catalyse the hydrolysis of ester bonds of triglycerides [2,3]. Cutinase is an industrially interesting molecule for its application in detergents as a fat stain removing enzyme [4]. During the assignment of the nuclear magnetic resonances of *F. solani pisi* cutinase it appeared that the amide proton of Ala^{32} has a strongly upfield-shifted resonance at 3.97 ppm, indicative of an amide-aromatic hydrogen bond [5]. Inspection of the crystal structure of cutinase [6] revealed that the amide proton of Ala^{32} makes contact with the indole ring of Trp^{69}. In solution the aromatic interaction was identified unambiguously to be with Trp^{69} by several nuclear Overhauser effects (NOEs) between Ala^{32} and Trp^{69} [5]. The amide-aromatic hydrogen bond between these residues appears to stabilise the N-terminal side of the central parallel β-sheet of cutinase [7].

The amide-aromatic hydrogen bond between Ala^{32} and Trp^{69} is an obvious candidate to explain the observed quenching of the tryptophan fluorescence signal of cutinase. If this interaction breaks upon irradiation, it would provide an explanation for the increase in fluorescence signal. Another possibility is that the fluorescence signal is quenched by the adjacent disulfide bond between Cys^{31} and Cys^{109}. However, at first sight it seems unlikely that a disulfide bond would break upon irradiation. The photo-induced process converting non-fluorescing into fluorescing molecules turned out to be irreversible, allowing us to study the irradiated species by slow methods like NMR spectroscopy and chemical detection of free thiol groups with a sulfhydryl reagent. We unambiguously show that the unusual fluorescence behaviour of Trp^{69} in cutinase is caused by a tryptophan mediated photoreduction of the disulfide bond between Cys^{31} and Cys^{109}, while the amide-aromatic hydrogen bond between Ala^{32} and Trp^{69} remains intact.

As supporting information, a table is provided with the backbone amide resonance assignments of irradiated cutinase (Table 1).

2. Materials and methods

2.1. Enzymes

Recombinant cutinase was produced in *Saccharomyces cerevisiae* and purified as described previously [8,9]. Recombinant, uniformly ^{15}N labelled cutinase was produced by using ^{15}N labelled ammonium sulfate (99% ^{15}N, Cambridge Isotope Laboratories) as the sole nitrogen source.

2.2. Irradiation of the samples and fluorescence measurements

The tryptophan excitation and fluorescence measurements were essentially performed as reported in Weisenborn et al. [1] and will be described only briefly below.

For the NMR measurements, lyophilised, uniformly ^{15}N labelled

*Corresponding author. Fax: +31 (10) 4605192.
E-mail: Rik.Pepermans@Unilever.com

[1] Present address: Department of Chemistry, Clark University, 950 Main Street, Worcester, MA 01610-1477, USA.

Abbreviations: NOE, nuclear Overhauser effect; NMR, nuclear magnetic resonance; HSQC, heteronuclear single-quantum coherence spectroscopy; FHSQC, fast HSQC; NOESY, nuclear Overhauser enhancement spectroscopy; TOCSY, total correlation spectroscopy; CSA, chemical shift anisotropy; TPPI, time proportional phase incrementation; DTNB, 5,5′-dithiobis(2-nitrobenzoic acid)

0014-5793/99/$20.00
PII: S0014-5793(99)00990-4

cutinase was dissolved to a concentration of 100 μM in 95% H_2O/5% D_2O (99.9% D), 10 mM deuterated sodium acetate (99.5% D), 100 mM NaCl, 0.02% sodium azide at pH 5.0. The sample was irradiated in a 3 ml quartz cuvette (1 cm path length) using a Spex Fluoromax spectrofluorimeter (Jobin-Yvon) equipped with a thermostated cuvette holder operated at 20°C. During irradiation the sample solution was stirred magnetically to maintain homogeneity in the solution. The excitation wavelength was set at 295 nm (slit 30 nm) and the fluorescence signal was measured at 340 nm (slit 4 nm) [1]. The sample was irradiated until the maximum fluorescence signal was obtained (10 min) and subsequently concentrated to a concentration of 0.5 mM with a Centricon-10 concentrator (Amicon).

Unlabelled cutinase was irradiated in the same buffer at a concentration of 0.5 mM using a Hitachi F-4500 spectrofluorimeter (Hitachi). Whereas the wavelengths were as above, the excitation slit was set at 10 nm and the emission slit at 1 nm. The increase of the cutinase tryptophan fluorescence signal as observed with the Spex Fluoromax spectrofluorimeter was reproduced with the Hitachi spectrophotometer. However, due to the lower excitation power and the smaller maximum excitation slit of the Hitachi spectrofluorimeter, the rate of fluorescence signal increase is much lower.

2.3. NMR spectroscopy

Two two-dimensional (2D) ^{15}N-^{1}H water flip-back fast HSQC (FHSQC) experiments [10], a 3D ^{15}N-edited NOESY-HSQC [11] with a mixing time of 100 ms, and a 3D ^{15}N-edited TOCSY-HSQC experiment using a mixing time of 30 ms were recorded on the irradiated, uniformly ^{15}N labelled cutinase sample for assignment purposes. In the NOESY-HSQC sequence a gradient pulse was added at the end of the mixing time to remove non-zero order coherences [12]. The TOCSY-HSQC sequence was based on the gradient-enhanced TOCSY experiment proposed by Fulton et al. [13], which was combined with the FHSQC sequence [10] in a manner identical to the NOESY-HSQC experiment.

The pulse sequence used to measure the transverse (R_2) relaxation rate constants of the backbone ^{15}N nuclei in the irradiated cutinase sample was based on that of Kay et al. [14], modified to eliminate cross-correlation between dipolar and chemical shift anisotropy (CSA) relaxation [15–17]. The indirect nitrogen evolution period followed by the INEPT transfer was concatenated into a semi-constant time ^{15}N evolution period. Gradients were used to suppress artifacts [18] and to aid in the removal of water by means of the WATERGATE sequence [19]. Additional water suppression was accomplished by a high-power spin-lock pulse [20]. A prescan recovery delay of 1 s was used. Spectra were recorded with relaxation periods of 3.5, 7.0, 10.5, 14.0, 21.1, 28.1, 42.1, 56.2, 70.2, 84.3, 119.4 and 165.1 ms consisting of Carr-Purcell-Meiboom-Gill pulse trains.

All experiments were performed on a Bruker 600 MHz AMX spectrometer equipped with a Bruker BLAX 300 W linear amplifier and a 5 mm inverse triple resonance probehead (^{1}H/^{15}N/^{13}C) with a self-shielded z-gradient coil. All experiments were carried out at 25°C (console readout). The spectral width was 1824 Hz in the ^{15}N dimension (folding-in some backbone resonances) and 7246 Hz in the ^{1}H dimension(s). The HSQC experiment was also recorded with a larger spectral width in the ^{15}N dimension (3102 Hz). The HSQC and R_2 experiments were recorded with 256 complex points in t_1 and 1024 complex points in t_2. The NOESY-HSQC and TOCSY-HSQC spectra contain 32 complex points in t_1, 98 complex points in t_2, and 1024 complex points in t_3. The HSQC experiments were recorded with 88 scans for each free induction decay, the R_2 experiments with 32 scans, the NOESY-HSQC with 24 scans, and the TOCSY-HSQC with 16 scans. Quadrature detection in the indirectly detected dimensions was accomplished using the States-TPPI acquisition method [21].

2.4. NMR data analysis

Spectra were processed and analysed on Silicon Graphics workstations, using the Triad software package (Tripos Inc.). Convolution filtering of the time-domain data with a Gaussian function was applied to the acquisition dimension of all spectra to suppress the water signal [22]. All dimensions were apodised using a squared-cosine-bell. The ^{15}N dimension of the 2D spectra was zero-filled to 1K points and in the 3D spectra it was zero-filled to 64 points. Linear prediction [23] and subsequent zero-filling was used to improve the digital resolution of the indirect proton dimension of the 3D spectra to a final size of 256 points.

Weighted averages of backbone amide ^{1}H and ^{15}N chemical shift differences were calculated according to Grzesiek et al. [24] as

$$\Delta\delta = [0.5(\Delta\delta_{HN}^2 + (\Delta\delta_N/5)^2)]^{1/2}. \quad (1)$$

The R_2 relaxation rate constants were calculated from peak volumes by fitting two-parameter single exponential functions to the experimental data using the SAS package (SAS Institute Inc.), applying the Levenburg–Marquardt algorithm [25,26]. Error estimates for the rates were obtained from the standard deviations of the curve fits.

2.5. Detection of free thiol groups with DTNB

Free thiol groups were detected with the sulfhydryl reagent 5,5′-dithiobis(2-nitrobenzoic acid) (DTNB) [27]. For this purpose, 100 μl of a 0.5 mM cutinase solution was added to 900 μl of freshly prepared buffer (25 mM Tris, pH 8.5) containing an excess of DTNB (200 μM), both before and after irradiation. The absorbance at 412 nm (TNB^{2-}: $\varepsilon_{412} = 13600\ M^{-1}\ cm^{-1}$) was subsequently measured using a Cary-3E spectrophotometer (Varian Associates). The time dependence of the photo-induced reaction was followed by taking a 100 μl sample of the 0.5 mM cutinase solution every 0.5 h during irradiation. The samples were subsequently analysed for free thiol groups as described above.

2.6. Mass spectrometry

An irradiated cutinase sample reacted with DTNB was desalted by gel filtration on a PD-10 column (Pharmacia) and subsequently analysed by electrospray mass spectrometry using a Quattro-II triple quadrupole mass spectrometer (Micromass).

3. Results

3.1. Unusual fluorescence behaviour of cutinase

Weisenborn et al. [1] showed that irradiation of *F. solani pisi* cutinase in the tryptophan absorption band causes an increase of the fluorescence quantum yield by an order of magnitude, followed by a much slower decrease due to photo-bleaching. These results were reproduced. However, the rate of fluorescence signal increase appeared to depend strongly on the excitation power of the spectrofluorimeter and the width of the excitation slit. The photo-induced process converting non-fluorescing molecules into fluorescing molecules appeared to be irreversible: When a cutinase sample was irradiated until the maximum fluorescence signal intensity was reached and subsequently stored in the dark, it retained its increased fluorescence quantum yield (not shown). The buffer components were shown not to have any effect on the fluorescence properties of cutinase. Irradiation did not affect the activity of the enzyme measured on *p*-nitrophenyl-butyrate (not shown).

3.2. Assignment of irradiated cutinase

The irreversibility of the photo-induced process leading to an increased fluorescence quantum yield allowed us to study the irradiated species by NMR. For this purpose, a uniformly ^{15}N labelled cutinase sample was irradiated until the maximum fluorescence signal intensity was reached and subsequently subjected to NMR measurements. Compared to the ^{15}N-^{1}H HSQC spectrum of a normal, unirradiated cutinase sample [5], the HSQC spectrum of the irradiated sample shows a number of additional peaks, at the expense of the signal intensity of some 'normal' peaks (Fig. 1). From the peak volumes it was estimated that about 30% of the cutinase molecules in the irradiated sample have shifted signals. The shifted backbone amide resonances were identified with the help of the ^{15}N-edited TOCSY and NOESY spectra. All shifted amide signals in the irradiated cutinase sample could be assigned and the assignments are listed in the supporting

Table 1
Amide resonance assignments of irradiated cutinase[a]

Residue	$^{15}N^{b}$	$^{1}H^{Nb}$	$^{15}N^{c}$	$^{1}H^{Nc}$
Arg[17]	–	–		
Thr[18]	106.8	7.93		
Thr[19]	120.2	7.77		
Arg[20]	126.3	9.18		
Asp[21]	129.3	9.18	129.2	9.17
Asp[22]	116.5	7.71	116.5	7.69
Leu[23]	112.9	7.57	112.6	7.58
Ile[24]	119.9	7.50	119.1	7.51
Asn[25]	113.2	7.68	113.4	7.70
Gly[26]	109.9	6.87	109.6	6.84
Asn[27]	120.8	8.52	121.0	8.45
Ser[28]	119.3	9.06	118.8	9.07
Ala[29]	123.3	8.52	122.5	8.44
Ser[30]	113.8	8.04	112.1	7.74
Cys[31]	118.6	7.80	122.3	7.35
Ala[32]	122.5	3.95	102.0	3.75
Asp[33]	117.3	7.44	115.5	7.76
Val[34]	116.9	7.17	115.8	6.92
Ile[35]	125.7	8.60	125.3	8.29
Phe[36]	127.6	9.32	127.6	9.28
Ile[37]	127.3	7.99	127.1	7.94
Tyr[38]	125.4	8.00	125.4	8.03
Ala[39]	129.6	7.45	129.7	7.47
Arg[40]	–	–		
Gly[41]	106.2	9.65		
Ser[42]	–	–		
Thr[43]	–	–		
Glu[44]	118.8	7.51		
Thr[45]	115.5	8.94		
Gly[46]	107.9	8.18		
Asn[47]	114.1	8.21		
Leu[48]	117.0	9.03		
Gly[49]	110.1	8.26		
Thr[50]	–	–		
Leu[51]	120.6	8.25		
Gly[52]	103.1	6.64		
Pro[53]	–	–		
Ser[54]	113.4	7.01		
Ile[55]	121.7	7.16		
Ala[56]	119.4	8.26		
Ser[57]	111.4	8.03		
Asn[58]	120.3	7.14	120.3	7.13
Leu[59]	–	–		
Glu[60]	118.8	8.62	118.7	8.58
Ser[61]	114.4	7.69	114.3	7.70
Ala[62]	121.7	7.20		
Phe[63]	112.8	8.04	112.8	8.02
Gly[64]	110.0	7.73		
Lys[65]	121.1	8.56	121.3	8.55
Asp[66]	113.5	8.54	113.7	8.47
Gly[67]	106.8	7.73	107.3	7.78
Val[68]	116.2	7.30	116.1	7.60
Trp[69]	125.0	8.53	122.7	8.47
Ile[70]	123.8	9.99	123.3	9.89
Gln[71]	127.4	9.06	127.0	8.99
Gly[72]	112.6	8.07	112.5	8.04
Val[73]	119.8	8.40	120.0	8.46
Gly[74]	123.2	9.21	123.2	9.21
Gly[75]	113.7	8.53		
Ala[76]	129.1	9.01		
Tyr[77]	116.8	8.25		
Arg[78]	130.5	9.12		
Ala[79]	120.6	6.67		
Thr[80]	114.5	8.62		
Leu[81]	127.9	9.20		
Gly[82]	106.0	8.83		
Asp[83]	119.7	7.34		
Asn[84]	115.3	7.50		
Ala[85]	117.7	7.25		
Leu[86]	120.2	7.01		
Pro[87]	–	–		

Table 1 (*continued*)

Residue	$^{15}N^{b}$	$^{1}H^{Nb}$	$^{15}N^{c}$	$^{1}H^{Nc}$
Arg[88]	–	–		
Gly[89]	113.2	8.91		
Thr[90]	109.1	7.25		
Ser[91]	115.7	8.34		
Ser[92]	118.1	9.16		
Ala[93]	124.1	8.51		
Ala[94]	122.6	7.89		
Ile[95]	119.8	7.44		
Arg[96]	117.3	7.82		
Glu[97]	121.6	7.80		
Met[98]	119.9	8.18		
Leu[99]	119.8	8.97	119.8	8.95
Gly[100]	105.4	8.20	105.4	8.19
Leu[101]	123.3	7.72	123.3	7.73
Phe[102]	118.1	7.98	118.2	8.01
Gln[103]	116.8	8.30	116.8	8.23
Gln[104]	121.1	8.66	121.2	8.61
Ala[105]	121.7	8.49	122.4	8.50
Asn[106]	112.7	7.69	112.2	7.75
Thr[107]	111.6	8.05	111.6	7.91
Lys[108]	121.0	8.79	119.1	8.75
Cys[109]	111.8	7.77	113.9	7.88
Pro[110]	–	–		
Asp[111]	115.2	8.70	114.7	8.78
Ala[112]	123.9	7.62	123.1	7.79
Thr[113]	120.6	8.72	120.6	8.66
Leu[114]	125.2	7.83	125.4	7.96
Ile[115]	115.2	9.12	115.4	9.14
Ala[116]	120.7	8.42		
Gly[117]	103.3	8.08	103.2	8.06
Gly[118]	102.7	8.05		
Tyr[119]	122.3	7.55		
Ser[120]	126.6	9.15		
Gln[121]	–	–		
Gly[122]	107.1	8.58		
Ala[123]	123.5	7.59		
Ala[124]	120.7	7.40		
Leu[125]	120.3	8.80		
Ala[126]	123.0	8.32		
Ala[127]	116.4	7.93		
Ala[128]	119.9	8.18		
Ser[129]	111.6	8.38		
Ile[130]	120.1	8.03		
Glu[131]	121.9	8.01		
Asp[132]	117.5	7.32		
Leu[133]	124.5	7.33		
Asp[134]	120.2	7.89		
Ser[135]	122.3	8.91		
Ala[136]	122.5	8.39		
Ile[137]	115.1	7.31		
Arg[138]	121.0	8.22	121.1	8.25
Asp[139]	115.0	8.15	114.5	8.16
Lys[140]	116.8	7.68	116.5	7.64
Ile[141]	119.3	7.81	119.4	7.85
Ala142	137.3	9.42		
Gly[143]	98.7	6.99		
Thr[144]	117.0	9.21		
Val[145]	116.0	8.42		
Leu[146]	120.6	8.36		
Phe[147]	119.0	8.97		
Gly[148]	114.8	9.28		
Tyr[149]	113.9	5.74		
Thr[150]	119.8	6.91		
Lys[151]	114.3	5.34		
Asn[152]	118.9	6.91		
Leu[153]	120.1	8.70		
Gln[154]	121.3	9.70		
Asn[155]	112.6	8.14		
Arg[156]	120.8	7.96		
Gly[157]	103.1	9.26		
Arg[158]	116.2	7.36		
Ile[159]	124.1	9.81		

Table 1 (*continued*)

Residue	$^{15}N^{b}$	$^{1}H^{Nb}$	$^{15}N^{c}$	$^{1}H^{Nc}$
Pro[160]	–	–		
Asn[161]	110.6	8.21		
Tyr[162]	121.2	8.01	121.1	8.00
Pro[163]	–	–		
Ala[164]	129.4	8.98		
Asp[165]	113.3	8.50		
Arg[166]	115.4	6.91		
Thr[167]	116.5	8.02		
Lys[168]	127.6	8.28		
Val[169]	126.8	8.47		
Phe[170]	128.9	9.32		
Cys[171]	127.4	9.06		
Asn[172]	123.4	9.40		
Thr[173]	121.6	9.13		
Gly[174]	114.6	9.08		
Asp[175]	115.8	8.03		
Leu[176]	126.7	7.55		
Val[177]	112.4	7.49		
Cys[178]	115.2	7.68		
Thr[179]	109.2	7.62		
Gly[180]	107.9	8.04		
Ser[181]	113.7	7.41		
Leu[182]	121.5	8.40		
Ile[183]	122.2	7.71		
Val[184]	127.6	8.36		
Ala[185]	134.1	8.98		
Ala[186]	122.1	8.78		
Pro[187]	–	–		
His[188]	113.9	8.73		
Leu[189]	118.1	8.10		
Ala[190]	122.4	6.47		
Tyr[191]	117.6	8.30		
Gly[192]	110.0	8.73		
Pro[193]	–	–		
Asp[194]	116.9	7.38		
Ala[195]	122.6	7.93		
Arg[196]	108.6	7.08		
Gly[197]	103.9	7.04		
Pro[198]	–	–		
Ala[199]	118.2	8.72		
Pro[200]	–	–		
Glu[201]	115.5	7.65		
Phe[202]	119.9	7.85		
Leu[203]	116.5	7.60		
Ile[204]	118.5	8.80		
Glu[205]	118.7	7.98	118.7	8.00
Lys[206]	117.7	7.91	117.7	7.89
Val[207]	120.1	8.28		
Arg[208]	118.3	8.65	118.2	8.68
Ala[209]	119.6	7.76		
Val[210]	114.8	7.41	114.7	7.39
Arg[211]	–	–		
Gly[212]	108.1	7.95		
Ser[213]	115.0	8.11		
Ala[214]	130.9	7.97		

[a]H^{N} chemical shifts are expressed relative to TSP and ^{15}N chemical shifts are expressed relative to hypothetical internal liquid ammonia, by multiplying the ^{1}H TSP frequency by 0.101329118. All values are in ppm.

[b]Amide resonance assignments of the 'normal' cutinase species in the irradiated sample.

[c]Amide resonance assignments of the altered cutinase species in the irradiated sample. Values are only indicated when the assignments differ from the 'normal' cutinase species.

information. We did not try to increase the relative amount of the altered cutinase species by lengthening the irradiation time, as to minimise the effects of photo-bleaching and to minimise aggregation.

3.3. Comparison of backbone amide resonances

From Fig. 2 it can be seen that the backbone amide signals of the residues located around Trp[69] shift most upon irradiation. The remainder of the protein is not affected by irradiation in the tryptophan absorption band, indicating that the structural change is induced by the light absorption of Trp[69]. The effects of irradiation are most prominent in three regions of the primary sequence (Fig. 3): (1) the region around Cys[31] and Ala[32], the latter of which is involved in the amide-aromatic hydrogen bond with Trp[69]; (2) the residues around Trp[69] itself; and (3) the region around Cys[109], which makes a disulfide bond with Cys[31]. The amide ^{15}N resonance of Ala[32] is shifted downfield by as much as 10 ppm, which is the largest shift observed throughout the whole protein (Fig. 1). In contrast, the amide proton resonance of Ala[32], which is strongly upfield shifted in a normal cutinase sample (3.97 ppm) [5] due to its hydrogen bonding interaction with Trp[69], hardly changes upon irradiation (Fig. 1). The indole $N^{\varepsilon 1}H$ of Trp[69] also shifts only slightly upon irradiation (Fig. 1).

3.4. ^{15}N R_2 relaxation rates

In contrast to the longitudinal relaxation rate (R_1) and the heteronuclear NOE, the transverse relaxation rate (R_2) is sensitive to both internal motions on a ps–ns time scale and conformational exchange processes on a slower, μs–ms time scale. Furthermore, R_1 is less sensitive to ps–ns mobility than R_2, and the low sensitivity of the heteronuclear NOE experiment precludes NOE measurements at the low concentration of the altered cutinase species in the irradiated sample. Therefore, we measured the R_2 relaxation rates of the backbone ^{15}N nuclei in the irradiated cutinase sample. The values for the residues most affected by irradiation and with non-overlapping signals, and for the indole $^{15}N^{\varepsilon 1}$ of Trp[69] are shown in Fig. 4. The relaxation rates for both the normal and altered cutinase species in the irradiated sample are shown. The errors on the R_2 rates of the altered species are rather large, due to its low concentration ($\sim$0.15 mM). Still, within the precision of the measurements it can be concluded that irradiation of Trp[69] alters the internal dynamics in the affected region of the molecule. Residues 68, 107 and 108 have decreased R_2 values in the altered species, approaching the values for residues 29–33, which were shown to be flexible on the ps–ns time scale in native cutinase [7]. This suggests that the region around Trp[69] becomes more mobile upon irradiation.

3.5. Detection of free thiol groups

While native cutinase does not contain any free thiol groups, free thiols were detected with DTNB in irradiated cutinase samples. Thus, irradiation of the protein in the tryptophan absorption band causes the breaking of a disulfide bond. The irradiated cutinase molecules did not need to be unfolded to detect the thiol groups, indicating that they are freely accessible to DTNB. Fig. 5 shows the time dependence of the photo-induced reaction followed by fluorescence spectroscopy and the absorbance at 412 nm after reaction with DTNB. Both methods show a linear increase in signal, corroborating that the increase in fluorescence signal upon irradiation is caused by the breaking of a disulfide bond. Due to the high protein concentration (0.5 mM) and large sample volume (2 ml) needed for this experiment, only a small amount of cutinase molecules is converted after 4 h, which

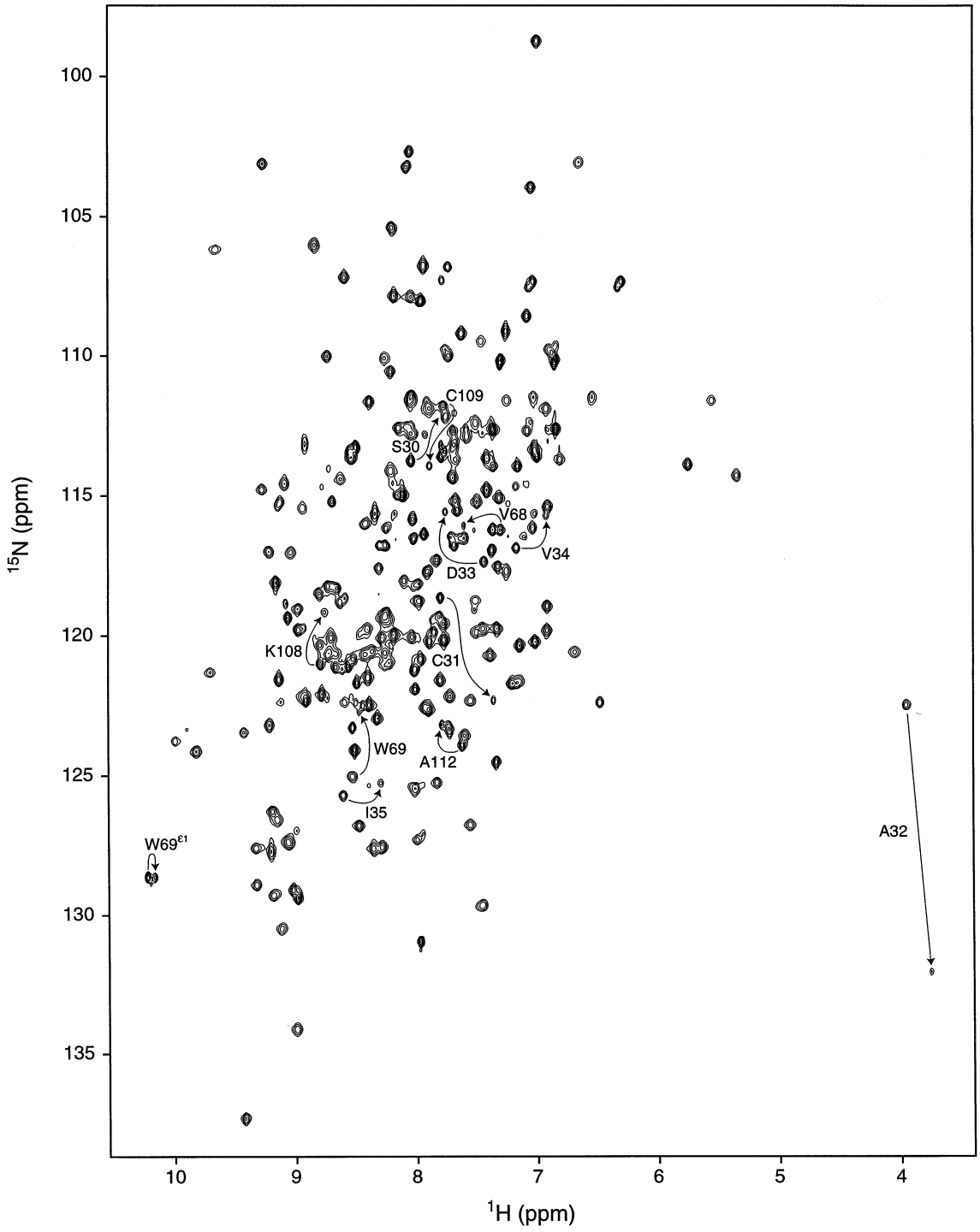

Fig. 1. 2D ^{15}N-^{1}H HSQC spectrum of the irradiated, uniformly ^{15}N labelled cutinase sample. Assignments are indicated for those residues which shift most upon irradiation using the one-letter amino acid code. The assignments of the indole N$^{\varepsilon 1}$H of Trp^{69} are also shown.

explains why the signal increase is linear and does not level off yet.

The electrospray mass spectrum of an irradiated cutinase sample reacted with DTNB shows two peaks (not shown). A native cutinase peak is observed at 20605 Da, which originates from the unchanged molecules. The second peak has an increased mass of 198 Da compared to the native peak, which corresponds to the mass of cutinase with one thiol group reacted with DTNB. Apparently, steric hindrance prevents the reaction of both thiol groups with the sulfhydryl reagent.

4. Discussion

The fluorescence signal of the single tryptophan residue (Trp^{69}) of *F. solani pisi* cutinase is highly quenched. Analysis of the distribution of the fluorescence lifetimes in a time-dependent experiment on the cutinase after a minimal irradia-

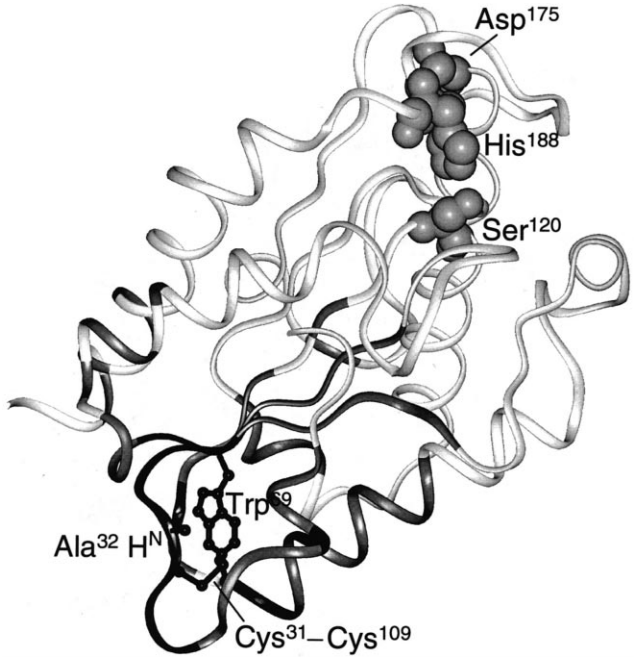

Fig. 2. Weighted averages of the differences in backbone amide ^{1}H and ^{15}N chemical shifts between the normal and altered cutinase species in the irradiated sample, mapped on the crystal structure of cutinase [6]. Prolines, residues with missing assignments or overlapping signals, and the N-terminal arginine, for which the difference could not be determined, as well as residues which did not shift upon irradiation are shown in white. Residues which did shift upon irradiation but with an average amide shift <0.1 ppm are represented in grey and residues with shifts ≥ 0.1 ppm are coloured black. The side chains of Trp^{69}, Cys^{31} and Cys^{109} and the backbone amide of Ala^{32}, involved in the amide-aromatic hydrogen bond with Trp^{69}, are shown in ball-and-stick, and the active site residues are shown in space filling representations. This figure was generated with the program Insight II (MSI).

tion yielded three lifetimes with corresponding weights [1]: 0.048 ns (0.93), 0.425 ns (0.02), and 4.3 ns (0.05). The preponderance of the very short lifetime results in the very low overall quantum yield. However, prolonged irradiation of the enzyme in the tryptophan absorption band causes an increase of the tryptophan fluorescence quantum yield by an order of magnitude [1]. Analysis of the distribution of the fluorescence lifetimes in a time-dependent experiment of cutinase after irradiation giving maximal conversion, yielded approximately the same three lifetimes, but with changed corresponding weights [1]: 0.047 ns (0.81), 0.345 ns (0.02), and 4.4 ns (0.17). A plausible interpretation of the increase of the overall quantum yield of the fluorescence is that the very fast decaying substate is converted into the slowly decaying one. Although it is not straightforward to interpret the weights of the lifetimes as populations of the substates, the weights of the very fast and slowly decaying lifetimes roughly correspond to the populations of the native and photo-reacted cutinase respectively. (The observation of the substate with the intermediate lifetime might be an artefact of the data analysis; T.J.W.G. Visser, personal communication.) In this study, we tried to elucidate the causes of the efficient quenching and its disappearance upon irradiation. The amide-aromatic hydrogen bond between Ala^{32} and Trp^{69} [5] might efficiently quench the tryptophan fluorescence signal of cutinase. As it is only about half the strength of a normal hydrogen bond [28], it is not inconceivable that this interaction would break upon irradiation, leading to an increase in fluorescence signal. Another possibility is that the fluorescence signal is quenched by the adjacent disulfide bond between Cys^{31} and Cys^{109}. This seems less plausible, as it would cost much more energy to break such a covalent interaction.

The NMR data of an irradiated, uniformly ^{15}N labelled cutinase sample indicate that the amide-aromatic hydrogen bond between Ala^{32} and Trp^{69} remains intact, as Ala^{32} retained its characteristic highly upfield-shifted amide proton

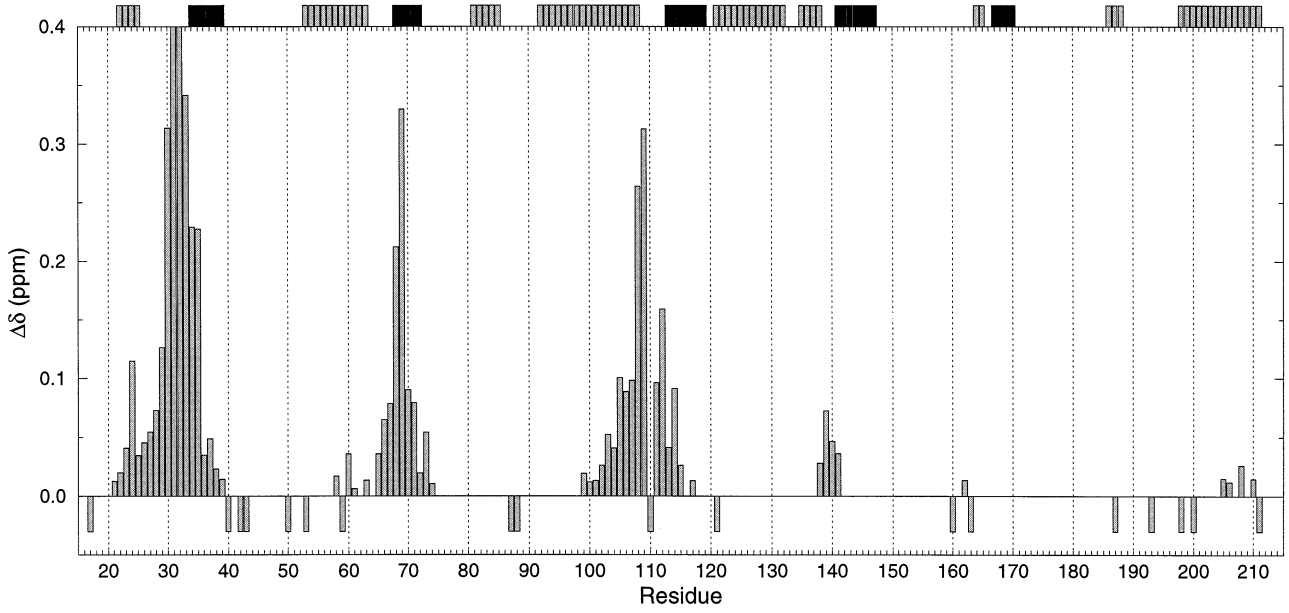

Fig. 3. Weighted averages of the differences in backbone amide ^{1}H and ^{15}N chemical shifts between the normal and altered cutinase species in the irradiated sample. Prolines, residues with missing assignments or overlapping signals, and the N-terminal arginine, for which the difference could not be determined, were given negative values. The average amide shifts of residues 31 and 32 run off the scale, but were 0.60 and 1.36 ppm, respectively. Residues in β-strands and helices are indicated by the black and grey bars, respectively, at the top of the figure.

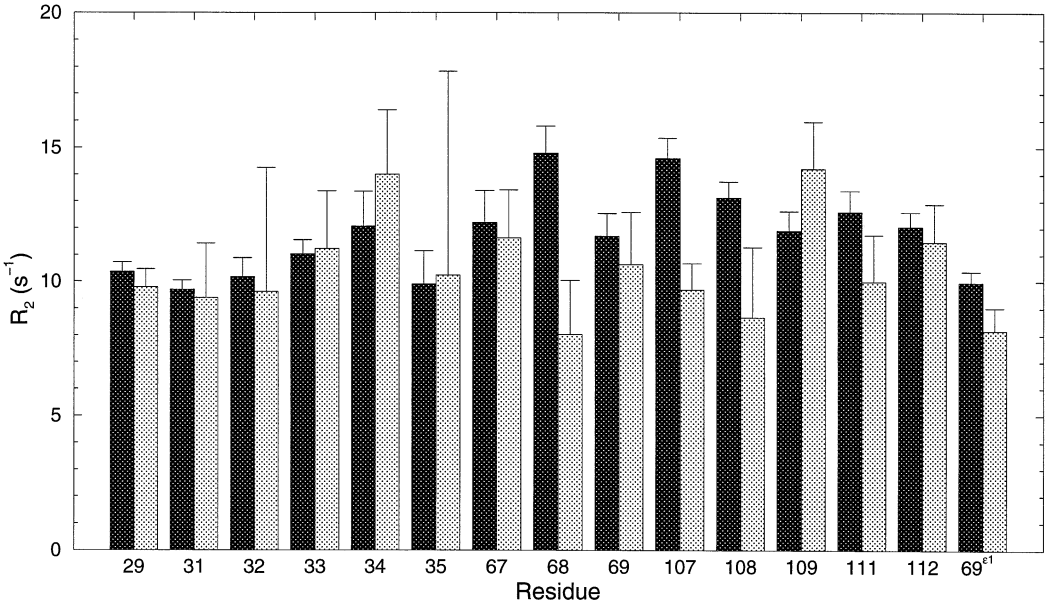

Fig. 4. R_2 relaxation rates of the backbone ^{15}N nuclei of the residues in cutinase most affected by irradiation and with non-overlapping signals, and of the indole $^{15}N^{\varepsilon 1}$ of Trp^{69} determined at 14.1 Tesla. The relaxation rates for the altered cutinase species in the irradiated sample are shown by the light bars and the relaxation rates for the unchanged cutinase molecules are shown by the dark bars for comparison.

resonance upon irradiation (Fig. 1). This interaction can therefore not explain the fluorescence behaviour of cutinase. Ala^{32} is positioned just before β-strand 34–39 and Trp^{69} lies in strand 68–72. In a previous study of the backbone dynamics of cutinase in solution [7], it was suggested that the amide-aromatic hydrogen bond between these residues might stabilise the N-terminal side of the β-sheet by anchoring the flexible loop 27–33 to the core of the protein. The alignment of the sequence of *F. solani pisi* cutinase to seven other cutinases [29–31] shows that *F. solani pisi* cutinase is the only cutinase so far with this type of amide-aromatic interaction. In six other cutinases the Trp at position 69 is conserved, but a Pro rather than an Ala is found at position 32. We can only postulate that in these cutinases the stabilisation is achieved by stacking of this Pro onto the Trp aromatic ring, as for none of these cutinases a 3D structure is available. Noteworthy, cutinase from *Aspergillus orizae* [31], the only cutinase so far that lacks the Trp at position 69, has an additional disulfide bond compared to the other cutinases, connecting helix 53–63 and strand 68–72. It might well be that this disulfide bond alternatively stabilises the N-terminal side of the β-sheet.

Chemical detection of free thiol groups with the sulfhydryl reagent DTNB and subsequent mass spectrometry showed that the increase of the tryptophan fluorescence signal of cutinase upon prolonged irradiation is accompanied by the breaking of a disulfide bond (Fig. 5). *F. solani pisi* cutinase contains four cysteines forming two disulfide bonds: Cys^{31}-Cys^{109} and Cys^{171}-Cys^{178}. The disulfide bond between Cys^{31} and Cys^{109} is in direct vicinity of Trp^{69}, while Cys^{171} and Cys^{178} are located in one of the two binding loops near the active site at the other side of the molecule. The NMR data showed that only the region around Trp^{69} is affected by irradiation (Fig. 2). Therefore, we can safely assume that the disulfide bond between Cys^{171} and Cys^{178} remains intact, but that the disulfide bond between Cys^{31} and Cys^{109} breaks upon tryptophan irradiation. The breaking of this disulfide bond increases the internal backbone mobility of residues 68, 107 and 108 (Fig. 4). Their dynamics becomes comparable to that of loop 27–33, which is a highly flexible loop in native cutinase [7]. Apparently, the fluorescence of Trp^{69} is quenched

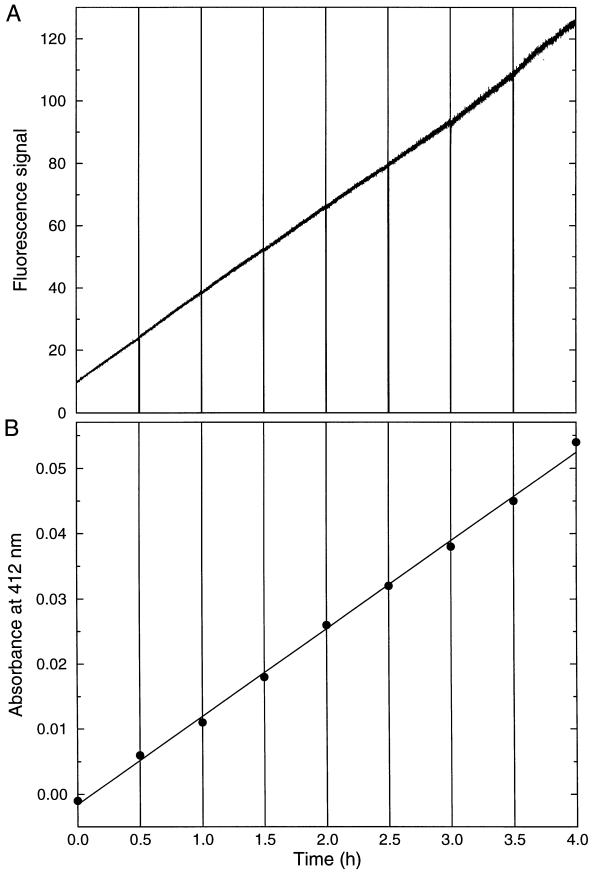

Fig. 5. Time course of the photo-induced reaction followed by (A) fluorescence spectroscopy and (B) the absorbance at 412 nm after reaction with DTNB.

by excited state electron transfer to the nearby cystine moiety, which is known to be a very strong quencher [32]. This was already suggested in [1]. The electron capture starts the reaction leading to the reduction of the cystine to a cysteine pair, which still quenches the fluorescence but much less efficiently [32]. Currently, we have no detailed explanation for the extreme downfield shift of the amide ^{15}N resonance of Ala^{32} upon irradiation, but it might be caused by a change in its π-electron density.

Tryptophan residues have been shown before to be redox-active amino acids. Tryptophan participates in the redox reaction of cytochrome *c* peroxidase [33] and in the flavin radical photoreduction of DNA photolyase [34,35]. In these examples, an excited state co-factor abstracts an electron from a tryptophan. In the case of cutinase, the tryptophan itself seems to be the excited species, donating electrons to the adjacent disulfide bond. To the best of our knowledge, this appears to be the first example of tryptophan mediated photoreduction of a disulfide bond in proteins.

Acknowledgements: J.J.P. was supported by a grant from Unilever Research. We thank A. Groenewegen for assistance with the NMR measurements, E.-J. Rutjes and M.C.D. van der Burg-Koorevaar for the production and purification of the uniformly ^{15}N labelled cutinase, H. Meder and E.J.J. van Velzen for assistance with the fluorescence measurements, S. de Jong for help with the SAS package, C.J. van Platerink and P.J.W. Schuyl for the electrospray mass spectrometry, and M. Merkx, W.F. Nieuwenhuizen, R. Hage, T.J.W.G. Visser, M.R. Egmond and a referee for useful suggestions.

References

[1] Weisenborn, P.C.M., Meder, H., Egmond, M.R., Visser, T.J.W.G. and van Hoek, A. (1996) Biophys. Chem. 58, 281–288.
[2] Kolattukudy, P.E. (1984) in: Lipases (Borgström, B. and Brockman, H.L., Eds.), pp. 471–504, Elsevier, Amsterdam.
[3] Lauwereys, M., de Geus, P., de Meutter, J., Stanssens, P. and Matthyssens, G. (1991) in: Lipases: Structure, Mechanism and Genetic Engineering (Alberghina, L., Schmid, R.D. and Verger, R., Eds.), Vol. 16, pp. 243–251, VCH, Weinheim.
[4] de Geus, P., Lauwereys, M. and Matthyssens, G. (1990) World Patent WO 90/09446.
[5] Prompers, J.J., Groenewegen, A., van Schaik, R.C., Pepermans, H.A.M. and Hilbers, C.W. (1997) Protein Sci. 6, 2375–2384.
[6] Martinez, C., de Geus, P., Lauwereys, M., Matthyssens, G. and Cambillau, C. (1992) Nature 356, 615–618.
[7] Prompers, J.J., Groenewegen, A., Hilbers, C.W. and Pepermans, H.A.M. (1999) Biochemistry 38, 5315–5327.
[8] van Gemeren, I.A., Musters, W., van den Hondel, C.A.M.J.J. and Verrips, C.T. (1995) J. Biotechnol. 40, 155–162.
[9] Nicolas, A., Egmond, M., Verrips, C.T., de Vlieg, J., Longhi, S., Cambillau, C. and Martinez, C. (1996) Biochemistry 35, 398–410.
[10] Mori, S., Abeygunawardana, C., Johnson, M.O. and van Zijl, P.C.M. (1995) J. Magn. Reson. Ser. B 108, 94–98.
[11] Talluri, S. and Wagner, G. (1996) J. Magn. Reson. Ser. B 112, 200–205.
[12] Jahnke, W., Baur, M., Gemmecker, G. and Kessler, H. (1995) J. Magn. Reson. Ser. B 106, 86–88.
[13] Fulton, D.B., Hrabal, R. and Ni, F. (1996) J. Biomol. NMR 8, 213–218.
[14] Kay, L.E., Torchia, D.A. and Bax, A. (1989) Biochemistry 28, 8972–8979.
[15] Boyd, J., Hommel, U. and Campbell, I.D. (1990) Chem. Phys. Lett. 175, 477–482.
[16] Kay, L.E., Nicholson, L.K., Delaglio, F., Bax, A. and Torchia, D.A. (1992) J. Magn. Reson. 97, 359–375.
[17] Palmer, A.G., Skelton III, N.J., Chazin, W.J., Wright, P.E. and Rance, M. (1992) Mol. Phys. 75, 699–711.
[18] Bax, A. and Pochapsky, S.S. (1992) J. Magn. Reson. 99, 638–643.
[19] Piotto, M., Saudek, V. and Sklenář, V. (1992) J. Biomol. NMR 2, 661–665.
[20] Messerle, B.A., Wider, G., Otting, G., Weber, C. and Wüthrich, K. (1989) J. Magn. Reson. 85, 608–613.
[21] Marion, D., Ikura, M., Tschudin, R. and Bax, A. (1989) J. Magn. Reson. 85, 393–399.
[22] Marion, D., Ikura, M. and Bax, A. (1989) J. Magn. Reson. 84, 425–430.
[23] Zhu, G. and Bax, A. (1990) J. Magn. Reson. 90, 405–410.
[24] Grzesiek, S., Bax, A., Hu, J.-S., Kaufman, J., Palmer, I., Stahl, S.J., Tjandra, N. and Wingfield, P.T. (1997) Protein Sci. 6, 1248–1263.
[25] Marquardt, D.W. (1963) J. Soc. Ind. Appl. Math. 11, 431–441.
[26] Press, W.H., Flannery, B.P., Teukolsky, S.A. and Vetterling, W.T. (1986) Numerical Recipes - The Art of Scientific Computing, Cambridge University Press, Cambridge.
[27] Ellman, G.L. (1959) Arch. Biochem. Biophys. 82, 70–77.
[28] Levitt, M. and Perutz, M.F. (1988) J. Mol. Biol. 201, 751–754.
[29] Ettinger, W.F., Thukral, S.K. and Kolattukudy, P.E. (1987) Biochemistry 26, 7883–7892.
[30] Sweigard, J.A., Chumley, F.G. and Valent, B. (1992) Mol. Gen. Genet. 232, 174–182.
[31] Ohnishi, K., Toida, J., Nakazawa, H. and Sekiguchi, J. (1995) FEMS Microbiol. Lett. 126, 145–150.
[32] Chen, Y. and Barkley, M.D. (1998) Biochemistry 37, 9976–9982.
[33] Sivaraja, M., Goodin, D.B., Smith, M. and Hoffman, B.M. (1989) Science 245, 738–740.
[34] Li, Y.F., Heelis, P.F. and Sancar, A. (1991) Biochemistry 30, 6322–6329.
[35] Kim, S.-T., Sancar, A., Essenmacher, C. and Babcock, G.T. (1993) Proc. Natl. Acad. Sci. USA 90, 8023–8027.